Myocyte Enhancer Factor 2C: an Osteoblast Transcription Factor Identified by DMSO Enhanced Mineralization.

Alexandre S. Stephens[1], Sebastien R. Stephens [1], Carl Hobbs[2], Deitmar W. Hutmacher[3], Desa Bacic-Welsh[1], Maria Ann Woodruff[3], Nigel A. Morrison[1*]

Running title: Mef2c involvement in osteoblast differentiation

[1] School of Medical Science, Griffith University, Gold Coast Campus, Queensland, 4215, Australia.
[2] Guy's Campus, Kings College, London.
[3] Institute for Health and Biomedical Innovation, Queensland University of Technology, Brisbane, Queensland, 4001, Australia

*Address correspondence to: Nigel A. Morrison, School of Medical Science, Griffith University, Gold Coast, Queensland, 4215, Australia. Tel: +61-7-55528330: Fax: +61-7-55528908; Email address: n.morrison@griffith.edu.au

Rapid mineralization of cultured osteoblasts could be a useful characteristic in stem-cell mediated therapies for fracture and other orthopaedic problems. Dimethyl sulfoxide (DMSO) is a small amphipathic solvent molecule capable of simulating cell differentiation. We report that, in primary human osteoblasts, DMSO dose-dependently enhanced the expression of osteoblast differentiation markers alkaline phosphatase (ALP) activity and extracellular matrix mineralization. Furthermore, similar DMSO mediated mineralization enhancement was observed in primary osteoblast-like cells differentiated from mouse mesenchymal cells derived from fat, a promising source of starter cells for cell-based therapy. Using a convenient mouse pre-osteoblast model cell line MC3T3-E1 we further investigated this phenomenon showing that numerous osteoblast-expressed genes were elevated in response to DMSO treatment and correlated with enhanced mineralization. Myocyte enhancer factor 2c (*Mef2c*) was identified as the transcription factor most induced by DMSO, among numerous DMSO-induced genes, suggesting a role for *Mef2c* in osteoblast gene regulation. Immunohistochemistry confirmed expression of *Mef2c* in osteoblast-like cells in mouse mandible, cortical and trabecular bone. shRNAi-mediated *Mef2c* gene silencing resulted in defective osteoblast differentiation, decreased ALP activity and matrix mineralization and knockdown of osteoblast specific gene expression, including osteocalcin and bone sialoprotein. Flow on knockdown of bone specific transcription factors, Runx2 and osterix by shRNAi knockdown of *Mef2c* suggests that *Mef2c* lies upstream of these two important factors in the cascade of gene expression in osteoblasts.

INTRODUCTION

Skeletal patterning and subsequent cellular differentiation during development is a complex process involving the activation and suppression of gene regulatory programs leading to bone formation (1). Once fully developed, bone remains a dynamic tissue by undergoing continual remodelling which functions to repair microarchitectural defects and maintain skeletal integrity (2). Numerous cell types are involved in the formation and homeostasis of the skeleton. Amongst these are osteoblasts (bone-forming cells) which differentiate from committed mesenchymal osteoprogenitor cells (1). The differentiation of osteoblasts is a highly coordinated process involving a clearly defined temporal sequence of events characterised by the commitment, proliferation and subsequent maturation of precursor cells into terminally differentiated osteoblasts (3,4). During this process, early differentiating cells undergo proliferation and secrete a collagen type 1-rich extracellular matrix. In the next phase, cellular proliferation decreases and the cells express factors involved in matrix maturation such as alkaline phosphatase. In the final stage, osteoblasts initiate matrix mineralization and express factors such as integrin binding sialoprotein and osteocalcin (3-5).

Osteoblast differentiation is tightly coordinated by the activities of transcriptional regulators; these include the master transcription factors RUNX2 and osterix (OSX) which govern the expression of genes involved in the developmental process (6). RUNX2 is indispensable for skeletal development and controls osteoblast differentiation by regulating the commitment of osteoprogenitors and activating major bone matrix genes (7). Osterix is also necessary for osteoblast differentiation and bone formation and functions downstream of RUNX2 (6). Other transcription factors with roles in osteoblasts include MSX2, DLX5, TWIST-1, AP1, ATF4, HOXA10 and ZFP521 (6-9).

Dimethyl sulfoxide (DMSO; $(CH_3)_2SO$) is a small, amphipathic molecule that is widely used as a solvent due to its abilities to dissolve both polar and non-polar compounds (10). Currently, DMSO is used as a cryo-preserving agent in cell banking (11) commonly at 10% concentrations that are then injected directly into the patient. Notably, DMSO is reported to stimulate osteoblast differentiation in MC3T3-E1, a mouse pre-osteoblast cell line, through ERK activation of transcription factors Runx2 and osterix (12).

In this study, we show that DMSO acts as a potent enhancer of human and mouse osteoblast differentiation as demonstrated by the significant gains in alkaline phosphatase (ALP) activity and mineralization observed throughout differentiation. Significantly, the effects of DMSO were anabolic in nature, such that the extent of matrix mineralization in DMSO-treated cells was greater than that of non-treated control cells, even when experiments were continued to the point where all cells were terminally differentiated. DMSO-enhanced osteoblast differentiation was used, in the model cell line MC3T3-E1, to identify novel genes involved in the developmental process. Unexpectedly, *Mef2c* was the transcription factor most potently induced by DMSO. *Mef2c* is a MADS-box transcription factor that is most commonly associated with the development and differentiation of the heart and skeletal muscle (13). Here, we show that *Mef2c* gene expression is dynamically regulated during osteoblast differentiation and that shRNA-mediated *Mef2c* gene silencing is associated with highly significant decreases in ALP activity, osteoblast gene expression and matrix mineralization, demonstrating a critical role for Mef2c in osteoblast differentiation.

MATERIALS AND METHODS

Cell culture and osteoblast differentiation - MC3T3-E1 cells (sub clone 14) were maintained in Minimum Essential Medium (α-MEM) (Invitrogen) containing 10% fetal bovine serum (FBS, Invitrogen), 1% penicillin/streptomycin solution (Invitrogen) and 1 mM sodium pyruvate (Invitrogen): this medium augmented with 50 µg/ml ascorbic acid and 10 mM beta-glycerophosphate was termed osteogenic medium (OM). For osteoblast differentiation, cells were seeded in 24-well culture plates at a density of 2.5×10^4 cells/well in a total volume of 0.5 ml of medium, then at 48 hours medium was replaced with OM with various concentrations of DMSO. Medium was changed every 72 hours unless stated otherwise. For calvarial osteoblast differentiation, calvaria obtained from new born mice were rinsed in phosphate buffered saline (PBS) and digested four times sequentially with 0.1% Collagenase A and 0.2% Dispase II (Roche) in PBS to liberate embedded cells. The pooled digestion solution was passed through a 70 µm cell strainer and cells were recovered via centrifugation. The cells were seeded into culture flasks containing α-MEM and grown for 3-4 days prior to osteoblast differentiation. Calvarial cells were prepared for osteoblast differentiation as per MC3T3-E1 cells. Human primary osteoblasts were obtained from biopsy material donated at orthopaedic procedures: bone was minced and washed in PBS, removing marrow and adipocytes and then treated with trypsin (Invitrogen) for 5 minutes. Pieces were then washed in PBS and osteoblasts permitted to grow out from explants in α-MEM with 10% FBS (Invitrogen). Mineralization and ALP assays were done as for MC3T3-E1 cells. Adipocyte derived mesenchymal cells were obtained from two hour collagenase digestion at 37ºC of excised, minced fat pads. Cells were washed in PBS and cultured in Dulbecco's Modified Eagle Medium (DMEM) with 5% FBS. 293T cells were maintained in DMEM containing 10% FBS (Invitrogen) and 1% penicillin-streptomycin solution (Invitrogen). All cells were maintained at 37ºC in a humidified atmosphere with 5% CO_2. DMSO concentrations are presented as percent volume. Procedures involving human samples were approved by the Queensland University of Technology

institutional committee. Procedures involving mice were approved by the animal ethics committee of Griffith University.

Alkaline phosphatase activity and matrix mineralization assays - ALP activity was assessed via the spectrophotometric quantitation of p-nitrophenol generated through the hydrolysis of p-nitrophenyl phosphate (pNPP). Briefly, cells were washed with one volume of PBS and lysed with the addition of 200 µl 50mM Tris-HCl, pH 8.0 and 0.5% Triton X-100 (per well, 24-well plate). 10 µl of cell lysate was incubated with 200 µl of 1 M diethanolamine, 0.5 mM $MgCl_2$, pH 9.8 containing 10 mM pNPP for 15-30 min. The reaction was stopped by the addition of 50 µl 3M NaOH and the absorbance was measured at 405 nm. Enzyme activity was standardized using purified calf intestinal ALP (NEB) and normalised to protein content as measured by the DC protein assay kit (Bio-Rad). ALP activity was expressed as nanomoles of pNPP converted per min per mg protein (nmole/min/mg protein). Matrix mineralization was assessed using Alizarin Red S staining according to Gregory *et al.* (14). Units are absorbance of solubilised Alizarin Red S measured at 405 nM per culture well. One A405 unit represents 2.96µMol Alizarin Red S precipitated per culture.

RNA extraction and cDNA synthesis - RNA was extracted from cells using the acid guanidinium thiocyanate-phenol-chloroform method (15). For cDNA synthesis, approximately 1 µg of total RNA was treated with DNAse I (Sigma) to remove any residual DNA and converted to cDNA using the ImProm-II reverse transcription system (Promega) according to the manufacturer's instructions. Reactions were carried out in 20 µl volumes and all cDNA samples were diluted 1:5 in DNAse-free water prior to real-time PCR.

Primers and quantitative PCR (qPCR) - PCR primers used in the study are listed in Table 1 and were designed from DNA sequences available through the Entrez Nucleotide database. Mouse gene nomenclature conventions are used (protein indicated by non-italics and gene names in italics). The specificities of candidate primer pairs were assessed by BLAST (www.ncbi.org) and BLAT analyses (genome.ucsd.edu). Primer pairs were selected that gave single amplification products using *in silico* PCR (genome.ucsd.edu). Specificity of amplification was verified by acrylamide gel electrophoresis, revealing a single fragment of the predicted size. qPCR amplifications were performed in an iCycler iQ Real-Time PCR Detection System (Bio-Rad) using the iQ SYBR green supermix (Bio-Rad). Reactions were carried out in total volumes of 20 µl and included 250 nM of each primer and 2 µl of diluted cDNA template containing 100 ng cDNA. The thermal cycler conditions were as follows: Step 1, 95 ºC for 2:30 min; Step 2, 95 ºC for 10 s, 59 ºC for 10 s and 72 ºC for 25 s (45 cycles); step 3, melt curve analysis from 59-95 ºC in 0.5 ºC increments. The specificity of the individual amplifications was assessed by the examination of the melt curves to confirm the presence of single gene-specific peaks of the characteristic melting temperature. Gene expression levels were normalised to the normalisation factor generated by the average of *Actb, B2m, Hmbs* and *Hprt1* internal control genes as determined by the GeNorm algorithm of Vandesomple et al. (16). Transcript levels are presented as fold change compared to zero time baseline levels.

Microarray analysis - Affymetrix and Illumina genechip microarray analysis was conducted at the Australian Genome Research Facility, Melbourne, Australia. For each sample, total RNA (10µg) underwent quality assessment by running a sample through an Agilent bioanalyzer prior to microarray processing and scanning.

Immunohistochemistry - C57BL/6J mice were either day 15 fetal or week 12 adult. Tissues were fixed in 4% paraformaldehyde/PBS, decalcified in 0.5M EDTA for 2 weeks, and embedded in paraffin. Five-micrometer sections were prepared for immunohistochemistry. Slides were blocked with 1% FBS for 10 minutes, then incubated for 2 hours at 21ºC with rabbit antiMEF2C primary antibody (Abcam, 64644) diluted 1:100 in buffered saline at a final concentration of 9 µg/ml, or with a nonimmune rabbit IgG (Santa Cruz Biotechnology) using the same final concentration, followed by rinses and addition of a biotinylated goat anti-rabbit IgG (Santa Cruz Biotechnology) for 30 min at room temperature. After incubation with streptavidin-horseradish peroxidase (DAKO) for 30 min at room temperature, slides were stained by exposure to DAB-liquid chromogen (DAKO) followed by counterstaining with Mayer's hematoxylin and mounted in Cytoseal 60 (Richard Allan Scientific). Positive antibody staining was identified by the presence of brown color.

shRNA constructs, retroviral particle production and infection - *Mef2c* shRNA sequence 1 (Sh1) was previously described (17). Sh2 and sh3 were designed using the Promega siRNA Target Designer (Version 1.51) in the mouse *Mef2c* mRNA. Sequence specificities were assessed via BLAST analysis. Forward and reverse oligonucleotides encoding the shRNA sequences (Table 1) were annealed via thermal cycling and cloned into the BamHI and EcoRI sites of pSIREN-RetroQ (Clontech). The pSIREN-RetroQ Luc vector (Clontech) which targets firefly luciferase was used as a control. Retroviral particle production was performed by co-transfection of pSIREN-RetroQ vectors, the VSV-G envelope glycoprotein vector pCSIG and the Friend MLV-based Gag-Pol expression vector pC57GP (18) in 293T cells using Fugene HD transfection reagent. Fresh medium was added to cells 24 hours post-transfection and viral supernatants were harvested a further 48 hours later. Viral supernatants were passed through a 0.45 μm pore size filter and used directly for infections. Infections were performed by seeding MC3T3-E1 cells at 2.5 x 10^5 cells in 25 cm^2 culture vessels. 24 hours later, the medium was replaced with viral supernatant containing 8 μg/ml polybrene. A further 24 hours later, infected cells were selected by replacing the viral supernatant with fresh medium containing 4 μg/ml puromycin. Infected cells were expanded in culture prior to use for subsequent analyses. Transient transfections were done using FuGene (Roche) according to the manufacturer's protocol. Mef2c expression vector was constructed in pBABE vector (Addgene) using mouse *Mef2c* coding region amplified from MC3T3-E1 cDNA. pOSLUC was made by inserting the 600base pairs of human osteocalcin promoter upstream of firefly luciferase in the pGLBasic vector (Promega). This construct contain Runx2, osterix and vitamin D receptor binding sites. *Renilla* luciferase was used as a control for transfection efficiency according to the Dual-Glo procedure (Promega). Phosphorylation status of kinases was assayed using RayBio Phospho-ELISA kits exactly according to the manufacturer's instructions.

Cellular proliferation assays - Cellular proliferation was assessed using the 3-(4,5-dimethylthiazol-2-yl)-2,5-diphenyltetrazolium bromide (MTT) method. MC3T3-E1 cells were seeded at 1 x 10^4 cells per well in 24-well culture plates and grown in osteogenic medium for 1 to 7 days. Cultures were gently washed once with warm PBS and fresh medium containing MTT to a final concentration of 0.5 mg/ml was added to the wells. After an incubation period of three hours, medium was removed and the dye solubilised via the addition of 200 μl of isopropanol containing 0.1 % sodium dodecyl sulfate and 0.04 N hydrochloric acid. The absorbance of the dye solution was measured at 570 nm.

Statistical analysis - ALP activity, ECM mineralization and cellular proliferation assays were assessed using Student's t-test or analysis of variance with LSD post-hoc tests. Analysis of variance of natural-log transformed gene expression data with LSD post-hoc tests was used to assess the significance of differences betweens means. For time course analysis the generalized linear model (GLM, SPSS) was used. Cycle threshold corrected for housekeeper genes was considered a normally distributed trait and used for statistical analysis. Significant differences were denoted by $p<0.01$. Error bars in graphs represent a standard error. In some cases where effects are obvious and substantial, p values are not presented.

RESULTS

DMSO promotes osteoblast differentiation – Primary human osteoblasts were cultured in OM supplemented with increasing concentration of DMSO, resulting in increased ALP activity (Fig. 1*A*) and enhanced mineral formation as detected using Alizarin red staining (Fig. 1*B*). Similarly, mouse mesenchymal cells derived from testicular fat pad cultured in OM, exhibited a similar dose response of increased ALP activity enhanced mineralization to DMSO supplementation (Fig. 1*C* and *D*, respectively).

The response of the pre-osteoblast model cell line, MC3T3-E1, to DMSO was characterised in detail for dose response of ALP activity and mineralization (at 12 days, Fig. 2*A* and 2*B*, respectively) and time course of response at 0.55% DMSO (Fig. 2*C* and 2*D*, respectively). Enzyme activity levels were maximally induced (2.9-fold) at 0.55% DMSO and gradually decreased at the two higher doses of 0.8 and 1.0%, although still significantly elevated compared to control. In parallel, a highly significant dose-dependent increase in ECM mineralization was also observed in response to DMSO treatment (Fig. 2*B*). The rise in mineralization paralleled ALP activity. As

expected, mineralization was not detected over the first five days of differentiation for either treatment group. By seven days, small amounts of mineralization were detectable in both groups with levels slightly greater in DMSO-treated cells. Beyond that time, DMSO-treated cells contained significantly more mineral than control cells at every time point and culminated in a 2.4-fold increase by day 21. These data indicated that DMSO exerted an anabolic effect on MC3T3-E1 osteoblast differentiation where cells contained significantly increased levels of ALP enzyme activity and deposited greater amounts of mineral in response to treatment.

Exposure of cells in OM to DMSO for the first three days of culture was sufficient for the maximal enhanced mineralization effect, as delayed addition did not result in increased mineralization (Fig. 2*E*). These data suggest a critical early time window of effect of DMSO on MC3T3-E1 cells. In the first two days DMSO did not have a significant effect on cellular proliferation; however, a minor suppression became apparent at three days that persisted as cells differentiated under the effect of DMSO and OM (Fig. 2*F*).

A critical early window of exposure to DMSO was observed, although the full mineralization effect in MC3T3-E1 cells developed over several days after this critical window. If DMSO had a direct inducing effect on bone specific promoters, increased gene induction might be expected within that 72 hour window. This was tested by transfecting a human osteocalcin promoter-luciferase construct into MC3T3-E1 cells, and culturing in OM for 48 hours. DMSO (2.5%) exposure was limited to the last 24 hours prior to harvest (at 72 hours after transfection) and assay in order minimise effects on proliferation and focus on transcription effects. Two known inducers of human osteocalcin, 1,25dihydroxyvitamin D_3 (VD3, 100nM) treatment and Runx2 expression vector co-transfection, were used as positive controls. VD3 activation depends on endogenous vitamin D receptor. As expected, VD3 induced the human osteocalcin promoter. In the absence of DMSO, maximal expression was seen with VD3 and Runx2 treatment (6.8-fold). In the presence of DMSO, a significant boost to induction was seen, up to 18.5-fold ($p<10^{-9}$, Fig. 2*G*). An increase in osteocalcin induction in MC3T3-E1 cells after 24 hours exposure to DMSO treatment (in OM) is consistent with additional transcription factors being available to enhance promoter activity.

Quantitative assays for the phosphorylation status of protein kinases across the first 30 hours in OM plus DMSO compared with OM found no convincing involvement of DMSO in ERK1/2, p38MAPK and JNK signalling pathways. Significant increases in phosphorylated signalling factors were seen after 30 hours, with 2.8-fold ($p=4.8x10^{-7}$), for phospho JNK, 1.8-fold ($p=7.8x10^{-5}$) for phospho ERK and only 1.4-fold ($p=8.6x10^{-6}$) for phospho p38MAPK. Significant effects of DMSO on phosphorylated kinases were observed for ERK ($p=0.009$) and JNK ($p=0.014$), however these were only minor decreases in DMSO treated cells (10% and 7% decreases for ERK and JNK, respectively). There were no significant effects on total kinase content between OM and OM plus DMSO treatments at any time point for ERK1/2, p38MAPK or JNK (data not shown), although total kinase increased over time. Finally we considered if the pool of phosphorylated kinase over total kinase changed according to DMSO: once again there were no significant DMSO related changes within 30 hours. Furthermore, experiments with inhibitors of these pathways at appropriate concentrations did not suggest a role for the following inhibitors and pathways in the DMSO effect: U0126 for the ERK1/2 pathway, SB203580 for the p38MAPK pathway and Ly-294002 for the PI3/AKT pathway. The p38MAPK inhibitor SB203580 is reported to inhibit osteoblast gene activation through phosphorylation of osterix (19). Consistent with this observation, SB203580 decreased ALP activity in a dose dependent manner in MC3T3-E1 cells grown in OM; however the DMSO enhancement was still proportional to the reduced ALP activity (Fig. 2*H*). Taken together these data suggest that the initial effects of DMSO action in osteoblasts occurs in a critical 72 hour window and may involve enhanced induction of osteocalcin at the transcriptional level (based on promoter transfection) but seems unlikely to involve p38MAPK, ERK1/2, JNK, or Pi3K/Akt at least within the first 30 hours. Those effects observed were either in the reverse sense to a DMSO mediated enhancement effect or were minor enough in magnitude as to be discounted.

DMSO treatment is associated with increased expression of osteoblast markers - DMSO was clearly able to enhance osteoblast differentiation as revealed by elevated ALP

activity and mineralization. We next set out to investigate the effects of DMSO on osteoblast gene expression. Accordingly, the expression of marker genes was assessed at multiple time points throughout osteoblast differentiation. Cells were grown in osteogenic conditions over a period of 19 days and were harvested for qPCR analysis of endogenous gene expression at numerous time points (Fig. 3). Gene expression was expressed as fold change in transcript levels, measured by qPCR, referenced to zero time.

Transcript levels for endogenous mouse osteocalcin (mouse gene *Bglap2*) were approximately doubled by DMSO treatment, reaching a peak at day 7 (Fig. 3*A*). Similar changes were seen in integrin binding sialoprotein (*Ibsp*, Fig. 3*B*), matrix metalloproteinase 13 (Fig. 3*C*) and the osteoclast differentiation factor, receptor activator of NFKappa-b ligand (*Rankl*, Fig. 3*D*). Not all extracellular matrix protein genes were induced by DMSO: dermatopontin (*Dpt*) was potently repressed by DMSO (Fig. 3*E*). The expression of osteoblast transcription factor, osterix (*Osx*, Fig. 3*F*), was significantly increased by DMSO treatment at three days, and showed increased transcript levels at later time points, suggesting that DMSO treatment results in an early and sustained increase in a key osteoblast specific transcription factor. The upregulation of osterix within 3 days may be sufficient to explain DMSO enhanced osteocalcin promoter activity in transfection (Fig. 2G) and the continued upregulation of osterix over 21 days may be sufficient to explain enhanced mineralization: further work is required to directly test such hypotheses. *Runx2* transcript levels were not significantly different at early time points between DMSO treated and control cells and, although *Runx2* transcript levels were higher in DMSO treated cells as *Runx2* increased over time, this was only nominally significant ($p=0.03$) at one time point (Fig. 2G).

Identification of genes super-induced by DMSO via genechip expression analysis and verification by qPCR - Differentiating MC3T3-E1 cells treated with DMSO clearly produced significantly greater amounts of mineralized matrix. One of the potential uses of DMSO-enhanced mineralization was to search for genes over-expressed as a consequence of DMSO treatment, effectively serving as a screening tool to identify novel genes involved in osteoblast differentiation and function. To search for genes super-induced by DMSO, we used affymetrix genechip microarrays to quantify gene expression in MC3T3-E1 cells grown under three different experimental conditions: standard medium which did not induce differentiation (non-mineralizing control); osteogenic medium which induced ECM mineralization (OM); and osteogenic medium supplemented with DMSO which produced highly mineralized matrix (OM plus DMSO). Cells were harvested for RNA extraction after twelve days of culture: this time point was chosen because four out of five osteoblast-expressed genes (*Osx*, *Ibsp*, *Mmp13* and osteocalcin) were significantly elevated as a consequence of DMSO treatment as reported above.

To identify DMSO super-induced genes, we applied two search filters to the microarray gene expression data. Firstly, all the genes that were at least moderately expressed (signal intensity over 100) and induced by more than 3-fold in OM relative to control were selected. These genes were further filtered by selecting only those which were a further increased more than 1.5-fold by DMSO. The filtering process resulted in the identification of 28 genes super-induced by DMSO (Table 2). DMSO treatment resulted in the super-induction of genes known to participate in bone biology such as osteoprotegerin (*Tnfrsf11b*) and integrin binding sialoprotein (*Ibsp*). Since osterix was induced by DMSO (Fig. 3*F*) we reasoned that any other transcription factor that is upregulated by DMSO in mineralizing MC3T3-E1 cells is a candidate for an osteoblast transcription factor with a role in mineralization. *Mef2c* transcription factor was identified as a DMSO super-induced gene on array.

Transcript profiling of Mef2c during osteoblast differentiation - To confirm the validity of the microarray results, we performed qPCR analysis in MC3T3-E1 cell experiments, to verify the expressions of *Ibsp* and *Mef2c* (Fig. 4*A* and 4*B*). Relative to the control cells cultured in αMEM, *Ibsp* expression was significantly induced 16-fold and 82-fold in OM and OM plus DMSO cultures, respectively, confirming the microarray. Similarly, *Mef2c* gene expression was upregulated 10-fold and 60-fold in OM and OM plus DMSO samples, respectively, relative to control. *Mef2c* gene expression was assessed during a time course of MC3T3-E1 differentiation (Fig. 4*C*), showing that *Mef2c* expression levels increased during the initial stages of differentiation, peaking at day seven before decreasing by day 13. *Mef2c* transcript

levels are induced up to 100-fold by culture in mineralizing medium. In cells treated with DMSO, the peak of *Mef2c* induction was earlier (5 rather than 7 days) and induction was more sustained at later time points. In these respects, the DMSO effect on *Mef2c* induction in MC3T3-E1 cells was similar to that observed for osterix (see Fig. 3*F*).

The induction of *Mef2c* was confirmed in mouse primary osteoblasts. Mouse calvarial osteoblasts were isolated and cultured in OM in the presence of DMSO. Similar to the results in MC3T3-E1 cells, *Mef2c* was induced in calvarial osteoblasts during culture in OM compared to control medium (Fig. 4*D*) and *Mef2c* expression was further enhanced by DMSO. Furthermore, DMSO enhanced mineralization by calvarial osteoblasts (Fig. 4*E*). These data confirm the cell line MC3T3-E1 as a reasonable model for Mef2c effects in osteoblasts. Furthermore, in order to verify that *Mef2c* has effects on osteoblast biology that occur in a manner independent of DMSO, the following experiments represented in figures 6 through 9 were done completely in the absence of DMSO in culture.

Mef2c expression in os*teoblasts in vivo* - Immunohistochemistry was used to detect Mef2c protein in mouse osteoblasts (Fig. 5). Positive staining was seen in 15 day fetal mouse skull (Fig. 5*A*) in the maxilla and mandible (Fig. 5*B* and *C*), where staining was found in association with developing bone and was stronger than in adjacent Meckel's cartilage (Fig. 5*C*). Cells immediately adjacent to the bone surface were positive for Mef2c (Fig. 5*D*). In adult mouse bone, positive staining was found in the growth plate associated with hypertrophic chondrocytes and cells lining bone in the cancellous region (Fig. 5*E*). In adult femoral cortical bone, similar positive cells lining the bone surface were observed (Fig. 5*F*). Staining was also observed in osteocyte-like cells in lacunae in adult cortical bone (Fig. 5*G*).

Mef2c gene silencing results in defective osteoblast differentiation – Mef2c expression in MC3T3-E1 cells followed a similar pattern to that of osterix and was enhanced by DMSO, suggesting Mef2c as a candidate bone transcription factor. This was tested using a Mef2c expression vector transfected into MC3T3-E1 cells. *Mef2c* mRNA levels were increased and significant increases in endogenous osteocalcin and *Isbp* transcript levels were observed (Fig. 6*A*, *B* and *C*). In a separate transfection, cultured over 16 days, significantly increased mineralization was observed in *Mef2c* transfected cells (Fig. 6D). Since *Mef2c* transfection elevated the expression of osteoblast genes, we would expect *Mef2c* knock down to have the reverse effect if the expression of osteocalcin and *Ibsp* is dependent on *Mef2c*. *Mef2c* expression was selectively knocked down using shRNAi-mediated gene silencing. One published (17) and two novel shRNAi sequences targeting three separate regions of the *Mef2c* sequence were designed and cloned into pSIREN-RetroQ (Sh1, Sh2 and Sh3). A shRNAi sequence targeting firefly luciferase mRNA was used as a control (Shlux). Pooled stably transfected MC3T3-E1 cell lines were generated via retroviral transduction and used in differentiation experiments.

Targeting of *Mef2c* transcripts with shRNA resulted in highly significant and consistent decreases in *Mef2c* expression levels throughout MC3T3-E1 osteoblast differentiation (Fig. 7*A*). The rank order of effectiveness of *Mef2c* shRNAs from least to most effective was Sh1, Sh2 then Sh3. Although these knock down cell lines had a slightly decreased rate of proliferation that was significant statistically (Fig. 7B), the magnitude of this effect was not large enough to explain observed biological effects. The impact of selectively reducing *Mef2c* expression levels on osteoblast differentiation was investigated. Targeting of *Mef2c* transcripts resulted in highly significant reduction in ALP activity (Fig. 7*C*), with one cell line, Sh3, showing almost total suppression. The accrual of mineral through the time course was dramatically suppressed (Fig. 7*D*) and a delay in the onset of visible bone nodule formation was observed (Fig. 7*E*). Highly significant reductions in mineral accrual occurred in all shRNA cell lines (Fig. 7*D* and *E*) culminating in up to 10-fold reduction by day 21.

The magnitude of decreased ALP activity was correlated to the potency of *Mef2c* silencing such that Sh3, which mediated the greatest reduction in *Mef2c* expression, produced the largest reduction in ALP activity, suggesting that ALP activity was dependent on *Mef2c* levels in the cells. However, suppression of mineralization appeared similar in all three knock-down cells lines.

Knock down of Mef2c transcript is associated with significant decreases in osteoblast gene expression - Knockdown of *Mef2c* clearly resulted in reduced mineralization and ALP activity. In order to determine if this

was due to a block in osteoblast differentiation (where lack of induction of osteoblast specific genes might be expected) or a block in mineralization due to the singular loss of ALP activity, gene expression of osteoblast marker genes was examined by qPCR. If Mef2c is necessary for the differentiation of osteoblasts, and acts as an osteoblast transcription factor, a flow-on knockdown of osteoblast related gene expression should be observed.

Osteoblast related genes *Ibsp* and osteocalcin, that were upregulated by DMSO, were strongly suppressed in anti-*Mef2c* shRNAi cell lines (Fig. 8*A* and *B*, respectively), and in a manner related to the extent of *Mef2c* knockdown. Cell line Sh3 had the most potent knockdown, with almost complete suppression of *Ibsp* and osteocalcin gene expression and flow on knockdown of *Mmp13* (Fig. 8*C*). Recall that in DMSO treated cells (see Fig 3), dermatopontin (*Dpt*) transcript levels were suppressed by DMSO treatment (in which *Mef2c* expression was increased). In the Sh3 cell line, in which *Mef2c* is almost completely suppressed, a potent time-dependent induction of dermatopontin message was observed during culture in OM (Fig. 8*D*), suggesting *Mef2c* is a negative regulator of dermatopontin. These data suggest that *Mef2c* knockdown, at least in Sh3 cells line, results in the inverse phenotype to that of DMSO treatment: inhibited mineralization coupled with a lack of ALP activity, failure to induce osteoblast marker genes and a strong induction of *Dpt*. Flow on knock down of osterix was significant in the comparison of control Shlux to all knock down cell lines (Sh1, $p=0.02$; Sh2, $p=0.02$, data not shown) and was strongest in Sh3 cell line ($p<10^{-6}$, Fig 8*E*). In Sh3 relative to Shlux, the knock down of osterix was significant at all time points including time zero ($p=1.0\text{x}10^{-4}$). Flow on knockdown of *Runx2* ($p=0.004$, Fig. 8*F*) was observed in Sh3: such flow on knock down suggests that Mef2c is upstream of these key transcription factors in the cascade of gene expression involved in osteoblast differentiation. Runx2 has an osteoblast specific isoform (Runx2-II, 20) driven off the upstream promoter: this message was also suppressed 12-fold in Sh3 relative to Shlux ($p=0.002$, data not shown) in a manner similar to the data for general Runx2 isoforms (Fig. 8*F*).

Gene expression in MC3T3-E1 cells with Mef2c knockdown - In order to verify the finding that osteoblast differentiation was blocked by *Mef2c* knockdown, we investigated the consequences of *Mef2c* gene silencing on the expression of genes in cells undergoing osteoblast differentiation. Shlux and Sh3 cells were induced to differentiate into osteoblasts via the addition of OM and were harvested 3, 10 and 19 days for microarray gene expression analysis.

Low signal data (<100) were rejected and genes considered of interest if they were either highly induced, had high signal value that varied between day 3 and 10 or was different comparing control Shlux to *Mef2c* knock down cell line Sh3. The difference expected in *Mef2c* transcript level due to knockdown was observed in the array data (Fig. 9*A*). The top ranked genes for the absolute difference between day 3 and day 10 in control Shlux cells during growth in OM were mouse osteocalcin (*Bglap2*) and osteocalcin related genes (*Bglap1* and *Bglap-rs1*). The next in rank were *Ibsp*, and *Mmp13*. The osteocalcin related genes (*Bglap1*, *Bglap2* and *Bglap-rs1*), *Ibsp* and *Mmp13* were also the top rank of strongly suppressed genes in array comparison between Sh3 (*Mef2c* knock down cell line, Fig. 9*B*, *C* and *D*) compared to Shlux, confirming that the array detected the same gene changes as seen previously using qPCR. These observations validated the array as a discovery tool to identify candidates for further work related to *Mef2c* action in osteoblasts. Regulated genes that are highly expressed on array and that were represented by multiple probes sets in the array platform are presented in Fig. 9. The parathyroid hormone receptor (*Pthr1*) was identified as increased by DMSO (Table 2): *Pthr1* was significantly increased during osteoblast differentiation in Shlux and was suppressed in Sh3 cell line (Fig. 9*E*) suggesting positive regulation of *Pthr1* by Mef2c. Collagen type 2 alpha 1 (*Col2a1*) was similarly affected by *Mef2c* knockdown (Fig. 9F). As expected, both *Runx2* and osterix transcripts were significantly reduced on the array (Fig. 9*G* and *H*), consistent with the analysis using qPCR (see Fig 8). Numerous other genes were affected by *Mef2c* knockdown, consistent with a global effect of Mef2c on gene expression in MC3T3-E1 cells. The data suggest that Mef2c transcription factor is required for appropriate expression of the suite of osteoblast-specific genes that characterizes the cell phenotype and ultimately results in mineralizing activity. Table 3 and 4 contain the genes displaying the largest fold changes in expression, regardless of magnitude of expression, between the two cell lines at each of the time points.

Finally, the osteocyte marker gene sclerostin (*Sost*) was also evaluated as the *Sost* promoter is a proposed target gene of Mef2c in osteocytes (21). In our hands, *Sost* expression was not detected in differentiating MC3T3-E1 cells, either with DMSO or not, or with *Mef2c* knockdown, in any experiment using qPCR, indicated by non-detected cycle threshold values (data not shown). No array probe set showed signal over background in any array experiment. The absence of sclerostin expression suggests that under any of the conditions reported in this study, MC3T3-E1 cells do not acquire an osteocyte phenotype.

DISCUSSION

In this study, we showed that DMSO treatment was able to stimulate mineralization of human osteoblasts in primary culture. Increasing the mineralization potential of such cells may be useful in tissue engineering for replacement of mineralized tissues. Similarly, primary adipose derived mesenchymal cells were stimulated by DMSO to produce more mineral, as were primary mouse calvarial cells, suggesting that DMSO enhancement is a general phenomenon applicable to osteoblast culture. We then used the pre-osteoblast cell line MC3T3-E1 to investigate DMSO enhance osteoblast differentiation and as a tool to identify novel regulators of differentiation. We first established the optimal DMSO concentration required to enhance differentiation through dose response curves. We next investigated the impacts of DMSO enhanced differentiation through time course experiments. The results showed that DMSO facilitated increases in ALP activity and mineralization and the increases were sustained throughout differentiation. It seems likely that DMSO treated cells achieved a heightened state of differentiation reflected by an enhanced capacity to mineralize the surrounding extracellular matrix. Cheung *et al.* (12) examined *Runx2* and osterix induction by DMSO in normal α–MEM medium at five days only; *Runx2* (1.89-fold) and osterix (1.39-fold) induction by DMSO was significant. In contrast, we examined the effect of DMSO on target gene expression using a number of target genes at numerous time points in osteogenic medium (OM); in particular, we observed strong induction of osterix by DMSO over the entire time period of mineralization, including day three and five. In addition, we defined *Mef2c* as a target of DMSO induction. A critical period of the first three days was seen where DMSO exposure was sufficient to generate the maximal enhancement, a fact that may prove useful in tissue engineering. Investigations of that three day period showed that endogenous osterix was significantly elevated at three days treatment with DMSO and that enhancement of a transfected osteocalcin promoter can occur within that period. Although the mechanism of DMSO effect remains to be elucidated, it seems likely that the mechanism will involve transcription factors. Further work is needed to fully define the early effects of DMSO on gene expression in osteoblasts. DMSO has other effects in bone biology. Zyuz'kov *et al.* (31) show that DMSO treatment (for 5 days at 2g/kg) via gastric tube in mice, results in a decrease of colony forming unit-fibroblast (CFU-F) derived from the stromal fraction in bone marrow cultures at eight days. We also tested DMSO on osteoclast differentiation and found profound stimulation, particularly in the size of osteoclasts (unpublished data). To our knowledge, no experiments have been reported specifically addressing bone anabolic effects of DMSO *in vivo*. A more complete analysis of the effects of DMSO on bone *in vivo* is warranted, as osteoblasts, osteoclasts and stromal cells may be affected by DMSO.

Gene expression studies revealed that osterix, *Ibsp*, osteocalcin and *Mmp13* were increased as a consequence of DMSO treatment and provided evidence that key regulators of osteoblast function were altered by DMSO, consistent with an enhanced state of osteoblast differentiation. Microarray analysis revealed Mef2c as a novel factor involved in osteoblast differentiation. Mef2c is a MADS-box transcription factor that has pleiotropic effects with examples including heart development (22), cardiac hypertrophy (23), myeloid cell fate (24), and skeletal muscle differentiation (25), among many other effects. In addition, the *Mef2c* locus has recently been linked genetically to human bone mineral density (26). More germane to bone mineralization are observations of Arnold *et al.* (27), using various conditional *Mef2c* knock out mice, that *Mef2c* is expressed in hypertrophic chondrocytes and is involved in endochondral ossification. Our *ex vivo* models suggest that *Mef2c* is not restricted to the chondrocyte, but functions as a key osteoblast transcription factor upstream of both Runx2 and osterix in osteoblasts. We detected reasonable

expression of *Col2a1*, at least in MC3T3-E1 cells by gene array. Sakai *et al.* (28) detected expression of the *Col2a1* promoter in mouse osteoblasts *in vivo*, using a β galactosidase indicator line (Rosa26) crossed with a *Col2A1* promoter driving CRE, suggesting some commonality between chondrocytes and osteoblasts. Arnold *et al.* (27) reported that the *Col2A1* promoter was regulated by Mef2c. Consistent with that fact, we observed flow-on knock down of *Col2A1* in *Mef2c* knock down cell lines. Combining these lines of evidence, it seems likely that Mef2c acts in osteoblasts as well as chondrocytes.

Transcript profiling revealed *Mef2c* was dynamically regulated during MC3T3-E1 osteoblast differentiation and increased during primary calvarial osteoblast differentiation. In MC3T3-E1 cells, two distinct peaks in *Mef2c* gene expression were observed and coincided with the developmentally relevant time points (see 29) of day seven, where the cells slow their proliferation and begin to differentiate and days 16-19, where cells enter the terminal stages of differentiation and actively mineralize. The addition of DMSO to the culture medium resulted in an accelerated pattern of *Mef2c* gene expression whereby the first peak in expression was earlier and the second peak more substantial. Notably, the expression of *Mef2c* during the terminal stages of differentiation (days 13-19) was significantly elevated in DMSO-treated cells introducing the possibility that Mef2c could function as a regulator of mineralization.

Immunohistochemical analysis showed Mef2c in embryonic and adult mouse in cells associated with bone. Although such cells were not formally identified as osteoblasts using other markers, it seems reasonable to conclude that osteoblasts express Mef2c. Furthermore, transfection of *Mef2c* expression vector into MC3T3-E1 cells resulted in increased osteocalcin transcript and increased alkaline phosphatase activity suggesting that Mef2c can function in osteoblasts. Short hairpin mediated gene knock down in MC3T3-E1 cells, confirmed the functional role for Mef2c in osteoblast differentiation. The consistent knock down of *Mef2c* mRNA levels was linked to potent reductions in ALP activity throughout differentiation. ALP participates in inorganic phosphate homeostasis and is associated with matrix vesicle mineralization (30). Therefore, it was not surprising to observe that mineralization was also disrupted in *Mef2c* shRNAi expressing cells. Furthermore, the key osteoblast specific gene, osteocalcin, was suppressed in *Mef2c* knock down cell lines and, of all genes assayed by gene array, the osteocalcin related gene cluster (*Bglap1, Bglap2 and Bglap-rs1*) were the top rank of genes altered by *Mef2c* knock down. The data suggest an essential role for Mef2c in regulating osteoblast differentiation.

A potential mechanism via which Mef2c could regulate osteoblast differentiation is controlling the expression of Runx2 and osterix, which were both significantly knocked down at the mRNA level as a flow on from *Mef2c* knock down. This possibility is strengthened by the fact that osteocalcin is known to be regulated directly by Runx2 and osterix. Further work is needed to determine if Mef2c has a direct or indirect effect on osteocalcin promoter. The comparative analysis of gene expression between Shlux and Sh3 cells using microarrays revealed many differentially regulated genes, consistent with Mef2c being necessary for the maintenance of osteoblast specific gene expression. Notably, the lowered expression of several known osteoblast regulators, (such as *Akp2, Ibsp, Mmp13,* and *Pthr1*) indicated Sh3 cells had a general inability to differentiate correctly.

We could not detect *Sost* expression using q-PCR or gene array, arguing strongly that the DMSO treated cells do not adopt an osteocyte-like phenotype. Mef2c is proposed to mediate the regulation of the Sost enhancer by PTH (21). In our study, *Mef2c* knock down resulted in flow on knock down of *Pthr1* (the PTH receptor), suggesting an alternative connection between Mef2c and PTH that may operate in osteoblasts. This can be clarified in future studies.

In conclusion, we have demonstrated that DMSO has profound effects on the differentiation of human osteoblasts, mouse adipocyte derived primary cells, mouse calvarial osteoblasts and the model cell line MC3T3-E1. Treatment with DMSO resulted in highly significant increases in ALP activity and mineral deposition in each of these osteoblastic cell models. We used DMSO-enhanced MC3T3-E1 differentiation as a tool to screen for factors involved in the developmental process. Our search identified Mef2c as a candidate osteoblast transcription factor, whose expression was verified in mouse primary calvarial cells. shRNAi-mediated gene silencing in MC3T3-E1 cells demonstrated that *Mef2c* was required for proper osteoblast differentiation and function.

Our data suggests Mef2c has an important role in osteoblast biology and is required for proper osteoblast differentiation and matrix mineralization. We suggest that Mef2c is a key osteoblast transcription factor, upstream of Runx2 and osterix, and worthy of further study in osteoblast biology. Combined with its role in chondrocyte hypertrophy, osteoblast biology (this study) and its presence in osteocytes, Mef2c is positive regulator of skeletal formation, mineralization and homeostasis at a number of levels.

Acknowledgements. This work was supported by grants from the National Health and Medical Research Council of Australia (NAM) and the Australian Research Council (DWH).

REFERENCES

1. Karsenty, G. (2003) *Nature* 423, 316-318
2. Hadjidakis, D.J., and Androulakis, II. (2006) *Ann. N.Y. Acad. Sci.* 1092, 385-396
3. Franceschi, R.T. (1999) *Crit. Rev. Oral. Biol. Med.* 10, 40-57
4. Weiss, A. J., Iqbal, J., Zaidi, N., and Mechanick, J. I. (2010) *Curr. Osteoporos Rep.* 8, 168-177
5. Aubin, J. E., Liu, F., Malaval, L., and Gupta, A. K. (1995) *Bone* 17, 77S-83S
6. Marie, P. J. (2008) *Arch. Biochem. Biophys.* 473, 98-105
7. Komori, T. (2006) *J. Cell. Biochem.* 99, 1233-1239
8. Hassan, M. Q., Tare, R., Lee, S. H., Mandeville, M., Weiner, B., Montecino, M., van Wijnen, A. J., Stein, J. L., Stein, G. S., and Lian, J. B. (2007) *Mol. Cell. Biol*. 27, 3337-3352
9. Wu, M., Hesse, E., Morvan, F., Zhang, J. P., Correa, D., Rowe, G. C., Kiviranta, R., Neff, L., Philbrick, W. M., Horne, W.C., and Baron, R. (2009) *Bone* 44, 528-536
10. Santos, N. C., Figueira-Coelho, J., Martins-Silva, J., and Saldanha, C. (2003) *Biochem. Pharmacol.* 65, 1035-1041
11. Woods, E. J., Perry, B. C., Hockema, J. J., Larson, L., Zhou, D., and Goebel, W. S. (2009) *Cryobiology* 59, 150-157
12. Cheung, W. M., Ng, W. W., and Kung, A. W. (2006) *FEBS Lett.* 580, 121-126
13. Potthoff, M. J., and Olson, E. N. (2007) *Development* 134, 4131-4140
14. Gregory C. A., Gunn W. G., Peister A., and Darwin J. Prockop D. A. (2004) *Anal. Biochem.* 329, 77–84.
15. Chomczynski, P., Sacchi, N. (1987) *Anal. Biochem.* 162, 156-159
16. Vandesompele, J., De Preter, K., Pattyn, F., Poppe, B., Van Roy, N., De Paepe, A., and Speleman, F. (2002) Genome Biol. 3, RESEARCH0034
17. Zang, M. X., Li, Y., Wang, H., Wang, J. B., and Jia, H. T. (2004) *J. Biol. Chem.* 279, 54258-54263
18. Lassaux, A., Sitbon, M., and Battini, J. L. (2005) *J. Virol.* 79, 6560-6564
19. Ortuño. M.J., Ruiz-Gaspà, S., Rodríguez-Carballo, E., Susperregui, A.R., Bartrons, R., Rosa, J.L. and Ventura, F. (2010) *J. Biol. Chem.* 285, 31985-31994
20. Xiao, Z., Awad, H. A., Liu, S., Mahlios, J., Zhang, S., Guilak, F., Mayo, M. S., and Quarles, L. D. (2005) *Dev. Biol.* 283, 345-356
21. Leupin, O., Kramer, I., Collette, N. M., Loots, G. G., Natt, F., Kneissel, M., and Keller, H. (2007) *J. Bone Miner. Res.* 22, 1957-1967
22. Bi, W., Drake, C. J., and Schwarz, J. J. (1999) *Dev. Biol.* 211, 255-267
23. Xu, J., Gong, N. L., Bodi, I., Aronow, B. J., Backx, P. H., and Molkentin, J. D. (2006) *J. Biol. Chem.* 281, 9152-9162
24. Schüler, A., Schwieger, M., Engelmann, A., Weber, K., Horn, S., Müller, U., Arnold, M. A., Olson, E. N., and Stocking, C. (2008) *Blood* 111, 4532-4541
25. Potthoff, M. J., Arnold, M. A., McAnally, J., Richardson, J. A., Bassel-Duby, R., and Olson, E. N. (2007) *Mol. Cell. Biol.* 27, 8143-8151
26. Rivadeneira, F., Styrkarsdottir, U., Estrada, K., Halldorsson, B. V., Hsu, Y. H., Richards, J. B., Zillikens, M. C., Kavvoura, F. K., Amin, N., Aulchenko, Y. S., Cupples, L. A., Deloukas, P., Demissie, S., Grundberg, E., Hofman, A., Kong, A., Karasik, D., van Meurs, J. B., Oostra, B., Pastinen, T., Pols, H. A., Sigurdsson, G., Soranzo, N., Thorleifsson, G., Thorsteinsdottir, U., Williams, F. M., Wilson, S. G., Zhou, Y., Ralston, S. H., van Duijn, C. M., Spector, T., Kiel, D. P., Stefansson, K., Ioannidis, J. P., and Uitterlinden, A. G. (2009) *Nat. Genet.* 41, 1199-1206
27. Arnold, M. A., Kim, Y., Czubryt, M. P., Phan, D., McAnally, J., Qi, X., Shelton, J. M., Richardson, J. A., Bassel-Duby, R., and Olson, E. N. (2007) *Dev. Cell.*12, 377-389
28. Sakaia, K., Hiripib, L., Glumoff, L., Brandaua, P., Eerolac, R., Vuorioc, E., Böszeb, Z., Fässlera R., and Aszódi, A. (2001) *Matrix Biol.* 19, 761-767
29. Quarles, L. D., Yohay, D. A., Lever, L. W., Caton, R., and Wenstrup R. J. (1992) *J. Bone Miner. Res.* 7, 683-692

30. Balcerzak, M., Hamade, E., Zhang, L., Pikula, S., Azzar, G., Radisson, J., Bandorowicz-Pikula, J., and Buchet, R. (2003) *Acta Biochim. Pol.* 50, 1019-1038
31. Zyuz'kov, G.N., Gur'yantseva, L.A., Simanina, E.V., Zhdanov, V.V., Dygai, A.M., and Goldberg, E.D. (2007) *Bull. Exp. Biol. Med.* 143, 535-538

FIGURE LEGENDS

Fig. 1. DMSO enhances alkaline phosphatase (ALP) activity and ECM mineralization in osteoblasts. Cultured human osteoblasts were grown for the times shown in αMEM (black columns), osteogenic medium (gray columns, OM) or OM supplemented with DMSO (striped and checked columns) and assessed for ALP activity (A) and ECM mineralization (B). Mouse adipocyte derived mesenchymal cells were cultured in a similar manner, with similar results including (C) increased ALP activity and (D) increased mineralization associated with DMSO treatment at the concentrations indicated. Data represent mean ± SEM of at least three independent samples.

Fig. 2. DMSO enhances alkaline phosphatase (ALP) activity and ECM mineralization of a model osteoblast cell line (MC3T3-E1). Differentiating MC3T3-E1 cells were treated with various concentrations of DMSO and assessed for ALP activity (A) and ECM mineralization (B). Insert photo in B shows mineral nodule formation, visualized using Alizarin Red S, with increasing DMSO at day 12. Levels of ALP activity (C) and ECM mineralization (D) during osteoblast differentiation time courses in control cultures (OM medium, black triangles) and OM plus DMSO treated cells (0.55 % DMSO, black squares). The time of exposure of cells to DMSO altered the mineralization outcome (E), with the first 3 days of culture being critical for the maximal effect of DMSO. (F) Cell proliferation was only mildly suppressed by DMSO: MC3T3-E1 cells were seeded at 1 x 10^4 cells per well in 24-well culture plates and treated with various concentrations of DMSO. The cells were grown over a period of four days and cellular proliferation was assessed on each day via the MTT method. (G) DMSO treatment in OM results in increased induction of transfected human osteocalcin promoter within the first 72 hour of exposure: human osteocalcin promoter driving luciferase (pOSLUC) was transfected into MC3T3-E1 cells and induction measured after 72 hours in OM alone (black columns) or OM with exposure to DMSO for the last 24 hours (gray columns). Treatments included cotransfection of 100ng Runx2 expression vector and/or treatment with 100nM 1,25dihydroxyvitamin D_3 (VD3) to induce the osteocalcin promoter. (H) DMSO enhancement of ALP activity in MC3T3-E1 is resistant to the p38MAPK inhibitor SB203580. Enhancement by DMSO still occurred from the lower basal level that results from inhibition of p38MAPK pathway by SB203580. Cell culture was 12 days. Error bars are ± SEM of at least three independent samples. P values omitted since effects are large.

Fig. 3. DMSO significantly increases the expression of osteoblast markers during differentiation. Osteogenic medium (OM, black circles, black line) was compared to OM plus 0.55% DMSO (gray circles, gray line). MC3T3-E1 cells were harvested at various time points during osteoblast differentiation for quantitative gene expression analysis of osteocalcin (OSC, graph A), integrin binding sialoprotein (IBSP, graph B), matrix metalloproteinase 13 (MMP13, graph C) and receptor activator of NFkappa-b ligand (RANKL, graphs D). Remarkably, dermatopontin (DPT, graph E) was completely repressed by DMSO in osteogenic medium, in comparison to OM control. The osteoblast transcription factor osterix (graph F), was significantly induced by DMSO most time points assessed, including 3 days. *Runx2* (graph G) was not significantly different early in DMSO treatment and although of greater magnitude in DMSO treated cells, was significantly different with respect to DMSO at day 10 only (asterisk, $p=0.03$). Data represent mean ± SEM of three independent samples. In graphs A-F, asterisks denote significantly different to OM (for that time point) at $p < 0.01$. Overall p values (not shown for each) of the treatment effect for DMSO were determined using the general linear model based analysis of variance and all were $<10^{-6}$, except for *Runx2* (graph G) which was not significant.

Fig. 4. DMSO treatment results in the super-induction of *Ibsp* and *Mef2c* gene expression in osteogenic medium (graphs A and B, respectively). Cells were grown in αMEM (MEM, black columns), osteogenic medium (OM, gray columns) and osteogenic medium supplemented with 0.55% DMSO (DMSO, striped columns) for 12 days. Transcript profiling of *Mef2c* during osteoblast differentiation according to time (graph C) confirms sustained induction during osteoblast differentiation in OM (black circles) and super induction by DMSO addition in OM (gray circles). *Mef2c* is induced during mouse calvarial cell cultures and shows super-induction with DMSO (graph

D): *Mef2c* transcript levels were compared in calvarial osteoblasts grown in αMEM (MEM, back diamonds, striped line), OM (black circles, black line) and OM plus 0.55% DMSO (DMSO, gray circles, gray line). Photograph (E), shows mineralization of mouse calvarial osteoblasts in αMEM (MEM), OM, and OM plus 0.55% DMSO (DMSO) indicating enhancement of mineralization effect in calvarial osteoblasts by exposure to DMSO. * denotes significantly increased compared to OM ($p < 0.01$). Other P values omitted since effects are large (graphs A and B).

Fig. 5. Mef2c is present in osteoblasts. A. Immunohistochemistry of day 15 embryonic mouse head (parasagittal section, A), showing immuno-reactivity (brown stain) in the mandible and the maxilla (boxes). B and C. Boxes in image A are shown in greater detail; staining is positive in the maxilla (B) and the mandible (C). Arrows indicate examples of positive stain associated with developing bone: Meckel's cartilage is indicated (m in C). Bars are 200μM. D. Increased magnification of arrow location in C shows numerous positive staining cells around the developing bone (bar is 20 μM). E. Analysis of adult mouse bone shows staining in the hypertrophic chondrocytes of the growth plate (white arrow) and in sites immediately adjacent to bone (black arrow). Bar is 100μM. F. Adult mouse cortical bone shows bone lining cells stain positive for Mef2c. G. Osteocytes in lacunae of cortical bone stain positive for Mef2c. Bars in F and G are 20μM.

Fig. 6. Knock in expression of *Mef2c* by transfection in MC3T3-E1 cells results in increased expression of *Mef2c* (graph A), osteocalcin (OSC, graph B) and integrin binding sialoprotein (IBSP, graph C). MC3T3-E1 cells were transfected and grown subsequently in OM for the specified time before harvest and assessment of mRNA levels by q-PCR. All genes are significantly increased by *Mef2c* transfection at 7 days ($p<0.001$). D. In a separate transfection experiment, cultured to 16 days, a significant increase in extracellular matrix mineralization was observed in *Mef2c* transfected cells compared with empty vector transfected control ($p=4x10^{-4}$).

Fig. 7. shRNA mediated silencing of *Mef2c* gene expression: graph A shows the effectiveness of knock down of *Mef2c* transcript levels in control (Shlux, black columns, a non target shRNA) compared with three cell lines, Sh1, Sh2 and Sh3 (gray, striped and checked columns, respectively) with varying levels of *Mef2c* knock down. Significant knock down was obtained at all time points with Sh3 cell line exhibiting the greatest extent of knock down (p values not included since effects are large). Knock down cell lines have a minor decrease in cell proliferation (B) that does not explain the extent of knock down of alkaline phosphatase (ALP) activity (graph C) or knock down of mineralization which is nearly total in all cell lines (graph D). Cell lines Sh1 and Sh2 that had very minor decrease in proliferation, still had major suppression of mineralization. In addition, the appearance of visible bone nodules (Alizarin Red S stain, image E) was delayed in *Mef2c* knock down cell lines.

Fig. 8. *Mef2c* knock down results in flow on knock down of osteoblast specific genes. qPCR was used to determine transcript levels for candidate osteoblast related genes. Those genes that were induced by DMSO were repressed by Mef2c knock down. Integrin binding sialoprotein (IBSP, graph A), osteocalcin (OCS, graph 2) were knocked down in a manner correlated with extend of *Mef2c* knockdown in Sh1, Sh2 and Sh3, compared with control Shlux. The most extreme knock down line Sh3, was then examined. Matrix metalloproteinase 13 (MMP13, graph C) showed flow-on knock down (graph C) and dermatopontin (DPT, graph D) showed the reverse effect: flow on gene induction resulting from *Mef2c* knock down, suggesting that Mef2c acts as a repressor of this gene. Comparing Mef2c knock down cell line Sh3 against control (Shlux) demonstrated similar flow-on knock down of osteoblast transcription factors osterix ($p=0.001$, OSX, graph E) and *Runx2* ($p=0.004$, RUNX2, graph F). Transcript levels are relative to zero time in OM, except for osterix which was different at zero time: that is, transcript levels of osterix were already detectably different prior to culture in OM. P values in experiments A to D are all $<10^{-6}$ for the overall effect in the generalized linear model.

Fig. 9. Differential expression of osteoblast related genes resulting from *Mef2c* knock down. Shlux and Sh3 cells were induced to differentiate into osteoblasts via the addition of OM. Cells were

harvested 3, 10 and 19 days in OM for whole-genome microarray gene expression analysis. Genes with large changes in absolute signal and with repeated probe sets on array are shown. Significant differences were observed for *Mef2c* (A, MEF2C), osteocalcin related sequences (Bglap-rs1, B), osteocalcin (OSC, C), integrin binding sialoprotein (IBSP, D), parathyroid hormone receptor (PTHR1, E), alpha 1 chain of type 2 collagen (COL2A1, F), transcription factors *Runx2* (RUNX2, G), and osterix (OSX, H). Transcript levels represent the microarray intensity values, error bars are SEM, significance was based on two factor ANOVA using all time points and all data values (p values are all <0.006 for effect of *Mef2c* knock down, except *Runx2* which has $p=0.03$).

TABLES

Table 1. Real-time qPCR primers used in the study and oligonucleotide sequences of Mef2c targeting shRNAs

Name		Forward (5'-3')	Reverse (5'-3')
Genes	***Accession No.***		
Ibsp	NM_008318	gcgtcactgaagcaggtg	cggtaagtgtcgccacgag
Mef2c	NM_025282	gctgagatacgcttagcacttgagt	cgggtctgtccaaacctctataca
Osc	NM_001032298	gcagacaccatgaggaccc	ggtctgatagctcgtcacaagc
Osx	NM_130458	tggaatgtaccccagtcctctcgac	ccaggccttgcacatattaagcatt
Runx2	NM_009820	cagtcacctcaggcatgtc	gcgtgctgccattcgag
Runx2-II	NM_009820	ccaggaagactgcaagaagg	tattcctgcatggactgtggtt
Actb	NM_007393	ctctggctcctagcaccatgaaga	gtaaaacgcagctcagtaacagtccg
B2m	NM_009735	ctgctacgtaacacagttccaccc	catgatgcttgatcacatgtctcg
Hmbs	NM_013551	gagtctagatggctcagatagcatgc	cctacagaccagttagcgcacatc
Hprt1	NM_013556	gaggagtcctgttgatgttgccag	ggctggcctataggctcatagtgc
Dpt	NM_001937	agatatacaccagcagacccaacag	catgggaaagggagaattatccttc
Sost	NM_024449	caaccagtcggagctcaaggactt	agtagagaccgcaggtccttctgc
shRNAs	***Nucleotide target region****		
Sh1	531-549	gatccgaatagtatgtctcctggtttcaagaga accaggagacatactattcttttg	aattcaaaaagaatagtatgtctcctggttctctt gaaaccaggagacatactattcg
Sh2	682-700	gatccggtaacctgaacaagaatattcaagag atattcttgttcaggttacctttttg	aattcaaaaaggtaacctgaacaagaatatct cttgaatattcttgttcaggttaccg
Sh3	236-254	gatccggacaaactcagacattgtttcaagag aacaatgtctgagtttgtccttttg	aattcaaaaaggacaaactcagacattgttctc ttgaaacaatgtctgagtttgtccg

*From ATG start codon of Mef2c mRNA (NM_025282). Ibsp, integrin binding sialoprotein; Mef2c, myocyte enhancer factor 2C; Osc, osteocalcin or bone gamma-carboxyglutamate protein 2; Osx, osterix or trans-acting transcription factor SP7; Runx2, runt related transcription factor 2; Actb, actin, beta; B2m, beta-2 microglobulin; Hmbs, hydroxymethylbilane synthase; Hprt1, hypoxanthine guanine phosphoribosyl transferase; Dpt, dermatopontin; Sost, sclerostin.

Table 2. Genes super-induced by DMSO in differentiating osteoblasts

Accession Number	Fold change OM/CT	Fold change DMSO/CT	Fold change DMSO/OM	Gene name	Gene
D17444.1	3.2	15.0	4.7	Soluble D-factor/LIF receptor	*Lifr*
NM_028943	14.0	54.9	3.9	Sphingomyelin synthase 2	*Sgms2*
NM_025282.1	5.5	21.1	3.8	Myocyte enhancer factor 2C	*Mef2c*
NM_013703.1	6.5	24.6	3.8	Very low density lipoprotein receptor	*Vldlr*
AK003671.1	27.7	100	3.7	Carbonic anhydrase 3	*Car3*
NM_080440	9.3	32.3	3.5	Solute carrier family 8 (sodium/calcium exchanger), member 3	*Slc8a3*
AB013898.1	3.1	10.5	3.5	Osteoclastogenesis inhibitory factor	*Tnfrsf11b*
BC004048.1	9.4	32.2	3.4	Wnt inhibitory factor 1	*Wif1*
BB042892	5.7	19.0	3.3	Ubiquitin-conjugating enzyme 8	*Ubce8*
BE370703	8.4	27.7	3.3	Neutrophil cytosolic factor 1	*Ncf1*
NM_153060	5.8	16.3	2.8	Spinster homolog 2	*Spns2*
BM240191	3.6	10.1	2.8	Rho-associated coiled-coil forming kinase 1	*Rock1*
BI964347	3.3	8.6	2.6	A disintegrin and metalloproteinase domain 12 (meltrin alpha)	*Adam12*
XM_907370	4.3	11.2	2.6	Collagen, type XXII, alpha 1	*Col22a1*
NM_021491	3.6	8.7	2.4	Sphingomyelin phosphodiesterase 3	*Smpd3*
NM_172454	10.0	23.6	2.	Pannexin 3	*Panx3*
NM_153170	4.1	9.7	2.3	Solute carrier family 36 (proton/amino acid symporter), member 2	*Slc36a2*
NM_001081064	3.7	8.0	2.2	PDZ domain containing 2	*Pdzd2*
L20232.1	21.2	42.8	2.0	Bone sialoprotein	*Ibsp*
NM_009760	2.9	5.6	2.0	BCL2/adenovirus E1B interacting protein 3	*Bnip3*
NM_011356	29.0	56.5	2.0	Frizzled-related protein	*Frzb*
NM_053083	3.0	5.8	1.9	lysyl oxidase-like 4	*Loxl4*
NM_016894	3.9	7.4	1.9	Receptor (calcitonin) activity modifying protein 1	*Ramp1*
NM_009331	5.0	9.5	1.9	Transcription factor 7, T-cell specific	*Tcf7*
NM_019738	3.8	7.2	1.9	Nuclear protein 1	*Nupr1*
NM_011199	4.1	6.9	1.7	Parathyroid hormone receptor	*Pth1r*
NM_030888	3.4	5.6	1.6	C1q and tumor necrosis factor related protein 3	*C1qtnf3*
NM_053088	32.6	52.4	1.6	Interferon induced transmembrane protein 5	*Ifitm5*

Results are shown as fold change in gene expression. Cells were cultured for 12 days post-induction of osteogenic differentiation. CT, control cells cultured in non-mineralising medium; OM, cells cultured in osteogenic medium; DMSO, cells cultured in osteogenic medium supplemented with DMSO.

Day 3			Day 10			Day 19		
Symbol	**Accession**	**Fold**	**Symbol**	**Accession**	**Fold**	**Symbol**	**Accession**	**Fold**
Ly6a	NM_010738	-3.9	Ccl7	NM_013654	-7.5	Ccl7	NM_013654	-7.1
Tnnc1	NM_009393	-3.2	Abi3bp	NM_178790	-4.6	Abi3bp	NM_178790	-5.9
Ly6c1	NM_010741	-3.2	Ly6a	NM_010738	-4.6	Ly6a	NM_010738	-5.1
Loc100047583	XM_001479138	-2.76	Scl0002547.1_9	scl0002547.1_9	-4.1	Nme7	NM_138314	-4.8
Tgm2	NM_009373	-2.7	Ifi27	NM_029803	-4.0	Txnip	NM_023719	-4.4
Gdpd2	NM_023608	-2.5	Txnip	NM_023719	-3.8	Ecrg4	NM_024283	-4.4
Pappa	NM_021362	-2.4	Ccl5	NM_013653	-3.7	Htra3	NM_030127	-4.2
6330406i15rik	NM_027519	-2.4	Dcn	NM_007833	-3.5	Atp1b1	NM_009721	-3.8
Wisp2	NM_016873	-2.3	Klra4	NM_010649	-3.5	Mfap4	NM_029568	-3.7
Nme7	NM_138314	-2.3	Ly6c1	NM_010741	-3.5	Papss1	NM_011863	-3.6
Loc382972	XM_356781	-2.3	1500015o10rik	NM_024283	-3.2	Robo1	NM_019413	-3.4
Idb4	AK041164	-2.2	Figf	NM_010216	-3.0	Ly6c1	NM_010741	-3.3
Ifit3	NM_010501	-2.2	Loc100038894	XM_001471776	-3.0	Chst2	NM_018763	-3.1
6330406i15rik	NM_027519	-2.2	Ccl2	NM_011333	-3.0	Htra1	NM_019564	-3.1
Ppap2b	NM_080555	-2.1	Tnn	NM_177839	-2.9	Mrgprf	NM_145379	-3.1
B230343a10rik	scl41403.1.1_37	-2.1	Lum	NM_008524	-2.9	Casp1	NM_009807	-3.0
Abca3	NM_013855	-2.1	Syt1	NM_009306	-2.9	Alox5ap	NM_009663	-3.0
Nme7	NM_138314	-2.1	Txnip	NM_001009935	-2.9	Il33	NM_133775	-3.0
Cdkl5	NM_001024624	-2.1	Cdkl5	NM_001024624	-2.9	Cxx1a	NM_024170	-3.0
Sdpr	NM_138741	-2.1	Id4	NM_031166	-2.8	Pigt	NM_133779	-2.9

Table 3. Genes displaying lowered expression in control cells (Shlux) compared to *Mef2c* shRNA knock down (Sh3) cells at days 3, 10 and 19 during osteoblast differentiation. Negative sign indicates repression, fold indicates change in Sh3 relative to Shlux.

Day 3			Day 10			Day 19		
Symbol	**Accession**	**Fold**	**Symbol**	**Accession**	**Fold**	**Symbol**	**Accession**	**Fold**
Panx3	NM_172454	10.6	Cdsn	NM_001008424	11.4	Spata19	NM_029299	14.2
Ibsp	NM_008318	7.1	Trib3	NM_175093	10.3	Timp4	NM_080639	13.8
Mest	NM_008590	4.5	Megf10	NM_00100197	9.9	Col10a1	NM_009925	10.4
Smpd3	NM_021491	4.4	Cox6a2	NM_009943	8.3	Panx3	NM_172454	7.7
Pthr1	NM_011199	4.3	Pthr1	NM_011199	8.0	Cox6a2	NM_009943	7.7
Ifitm5	NM_053088	4.2	Chac1	NM_026929	6.5	Trib3	NM_175093	7.4
H19	NR_001592	3.6	Sema7a	NM_011352	6.3	Megf10	NM_001001979	7.3
Tnfrsf19	NM_013869	3.5	Aldh1l2	NM_153543	6.2	Mef2c	NM_025282	6.7
Ramp1	NM_016894	3.4	Mef2c	NM_025282	6.1	Krt14	NM_016958	6.4
Mef2c	NM_025282	3.3	Panx3	NM_172454	6.0	Cdsn	NM_001008424	5.5
Tmem176b	NM_023056	3.2	Ptgis	NM_008968	5.7	Ptgis	NM_008968	5.1
Tnnc2	NM_009394	2.8	Col10a1	NM_009925	5.5	Fam180a	NM_173375	4.6
Nupr1	NM_019738	2.6	Nupr1	NM_019738	5.0	Fam20a	NM_153782	4.2
Timp4	NM_080639	2.5	Scx	NM_198885	5.0	Aldh1l2	NM_153543	4.1
Akp2	NM_007431	2.5	Ramp1	NM_016894	4.8	Loxl4	NM_053083	4.0
C1qtnf3	NM_030888	2.4	Fam180a	NM_173375	4.7	Ibsp	NM_008318	4.0
Tnc	NM_011607	2.3	Slc6a9	NM_008135	4.5	Gper	NM_029771	4.0
Sp7	NM_130458	2.3	Ddit3	NM_007837	4.4	Slc40a1	NM_016917	4.0
Srpx2	NM_026838	2.2	Fabp3	NM_010174	4.3	Chac1	NM_026929	3.6
Wif1	NM_011915	2.2	Fam20a	NM_153782	4.2	Unc5b	NM_029770.2	3.6

Table 4. Genes displaying increased expression in control cells (Shlux) compared to *Mef2c* shRNA knock down (Sh3) cells at days 3, 10 and 19 during osteoblast differentiation. Fold indicates change in Shlux relative to Sh3. Analysis is based on fold change.

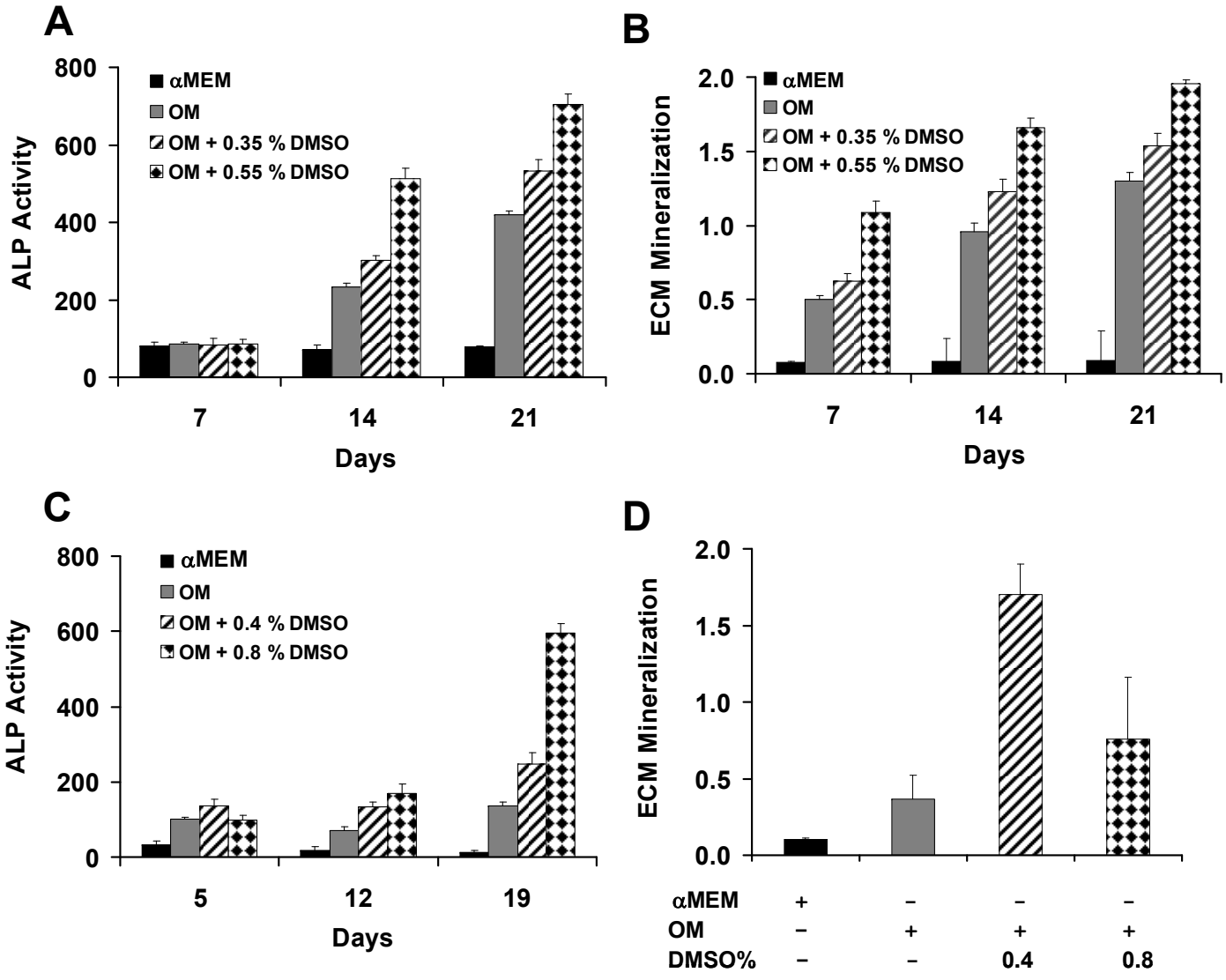

Figure 1 Stephens et al.

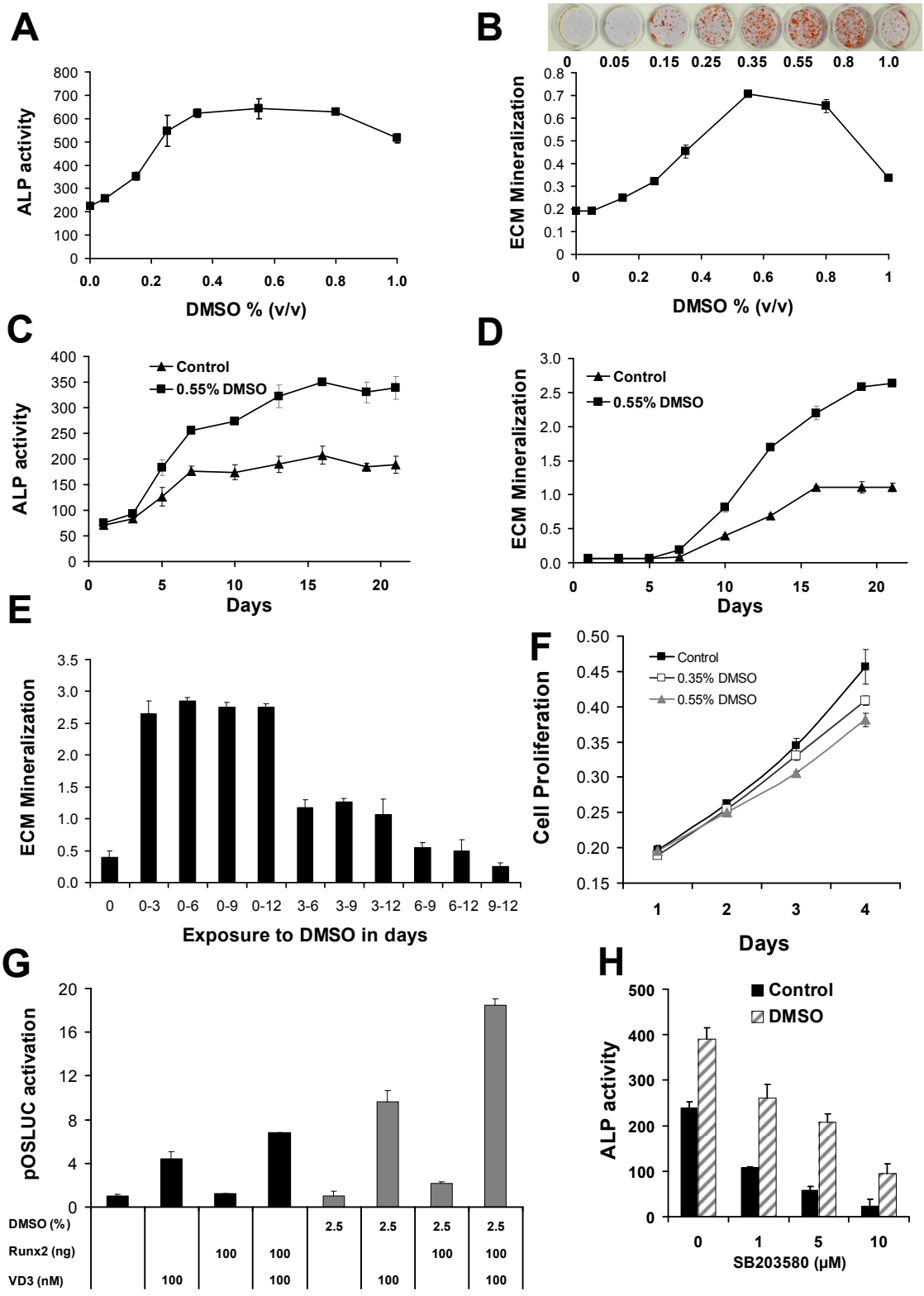

Figure 2 Stephens et al.

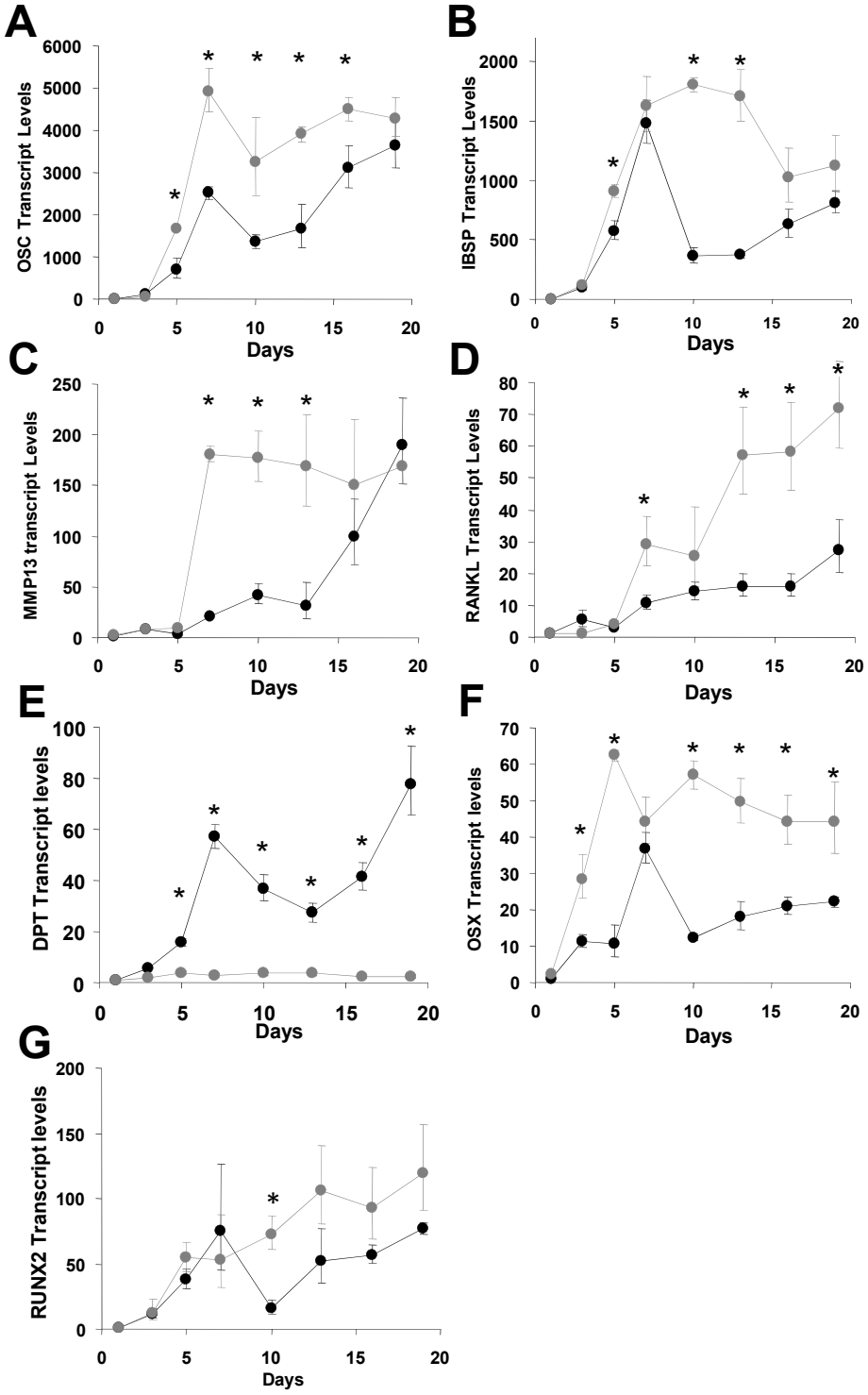

Stephens et al Fig 3.

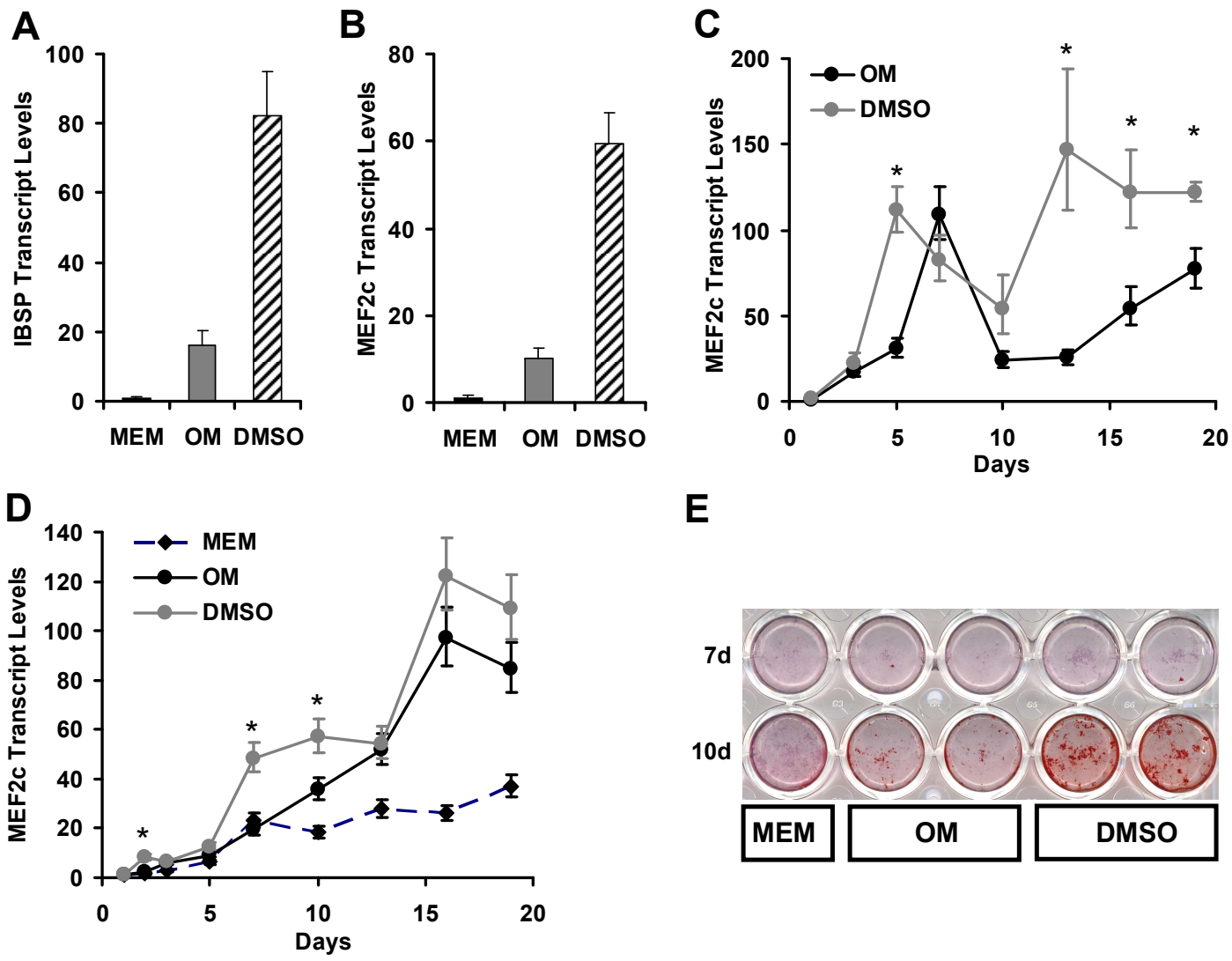

Figure 4 Stephens et al.

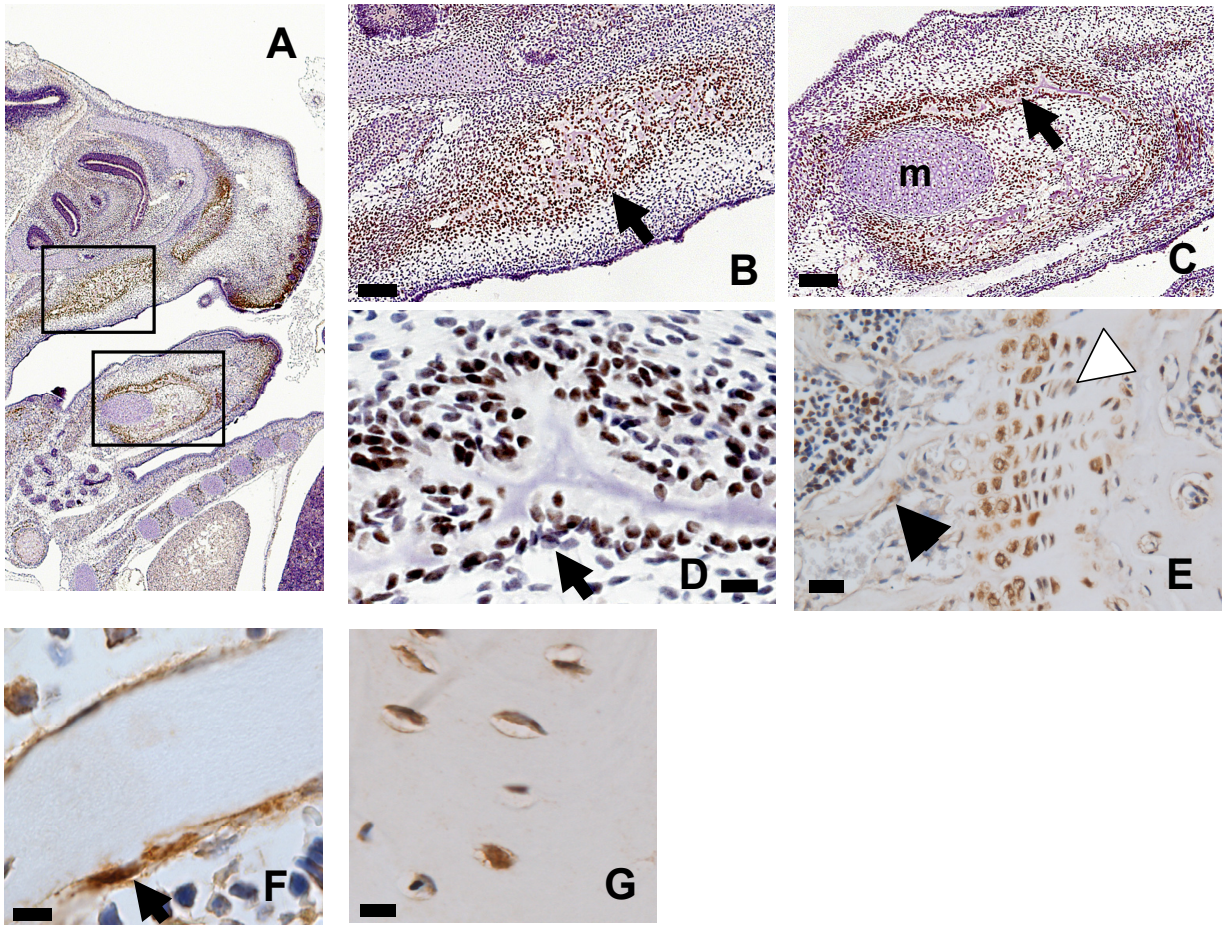

Figure 5 Stephens et al.

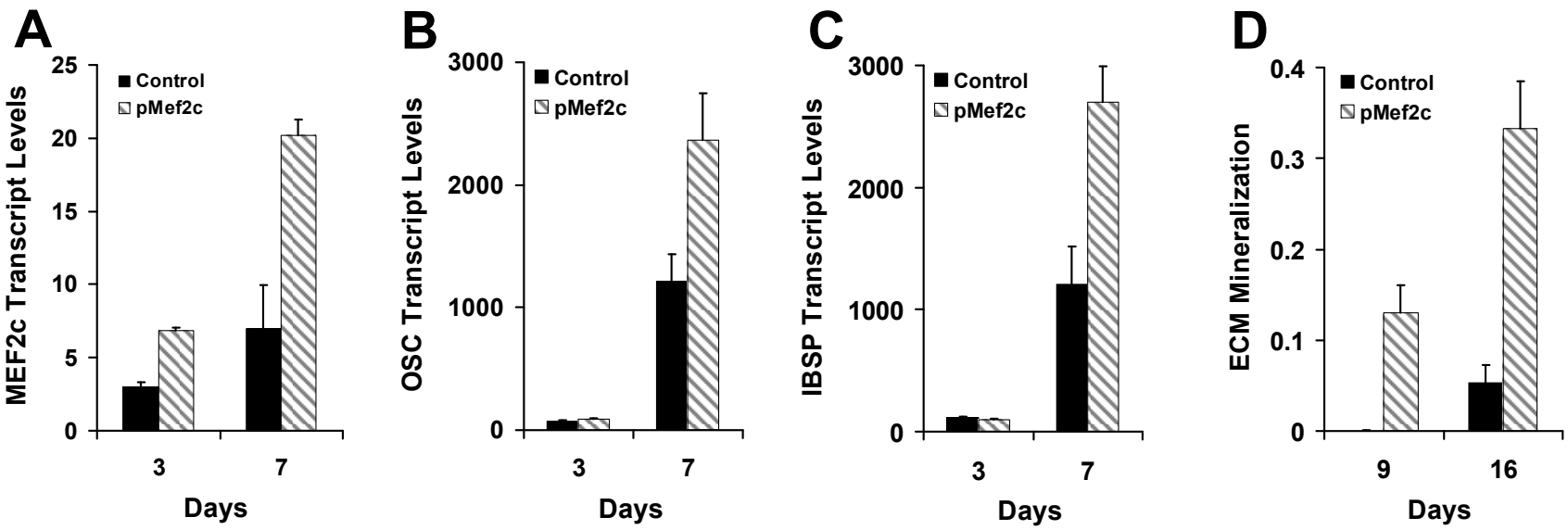

Figure 6 Stephens et al.

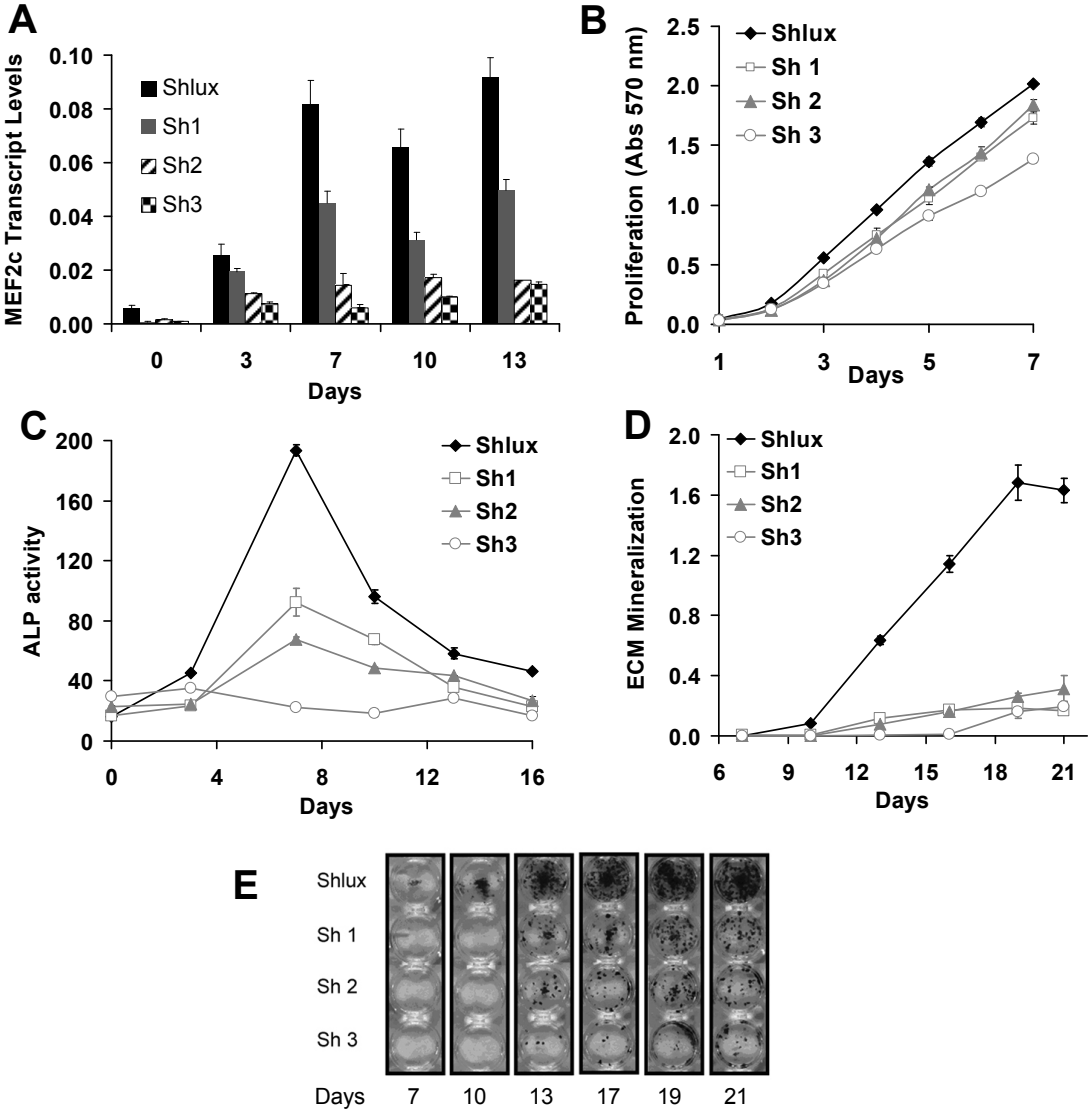

Figure 7 Stephens et al.

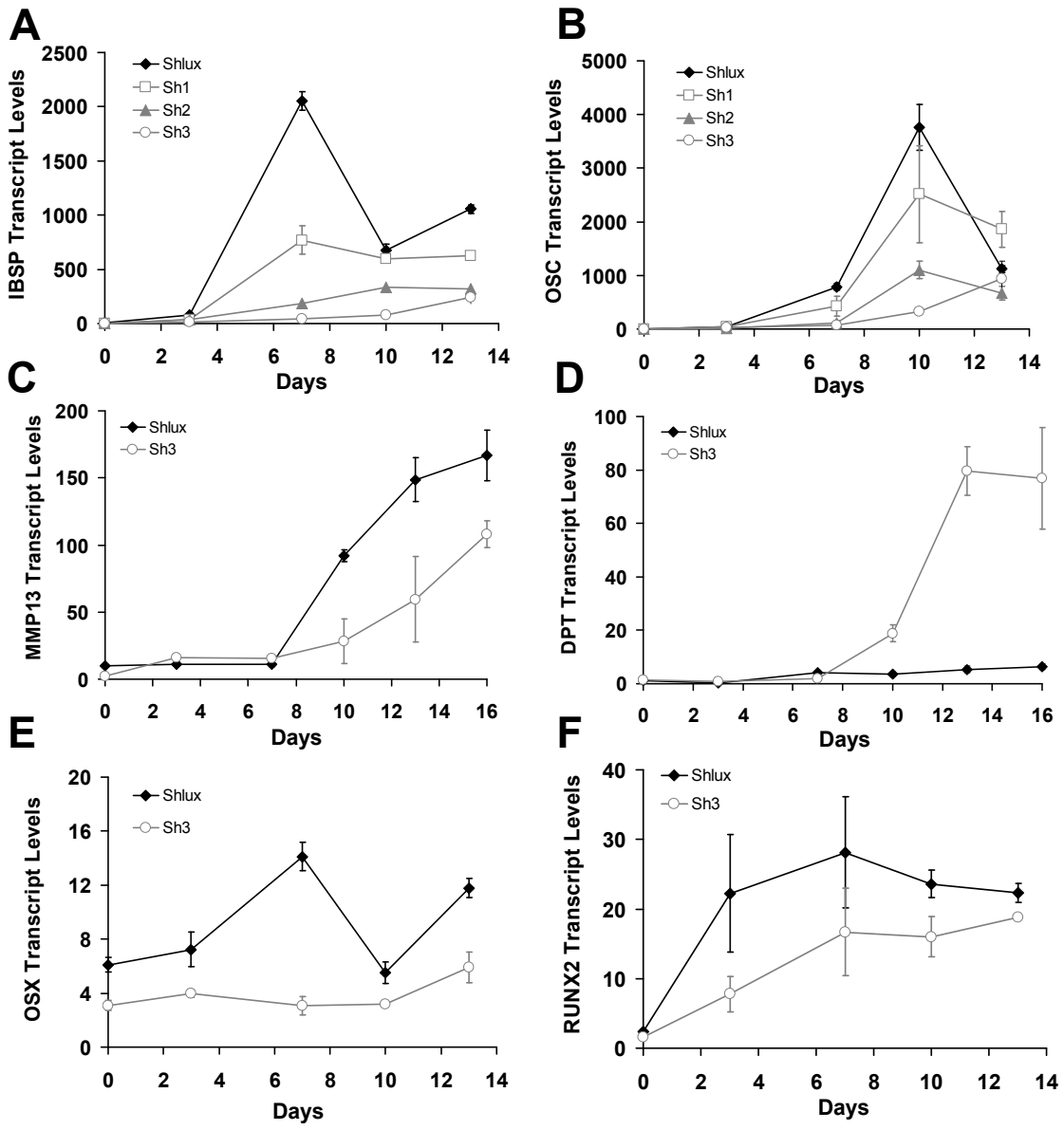

Figure 8 Stephens et al.

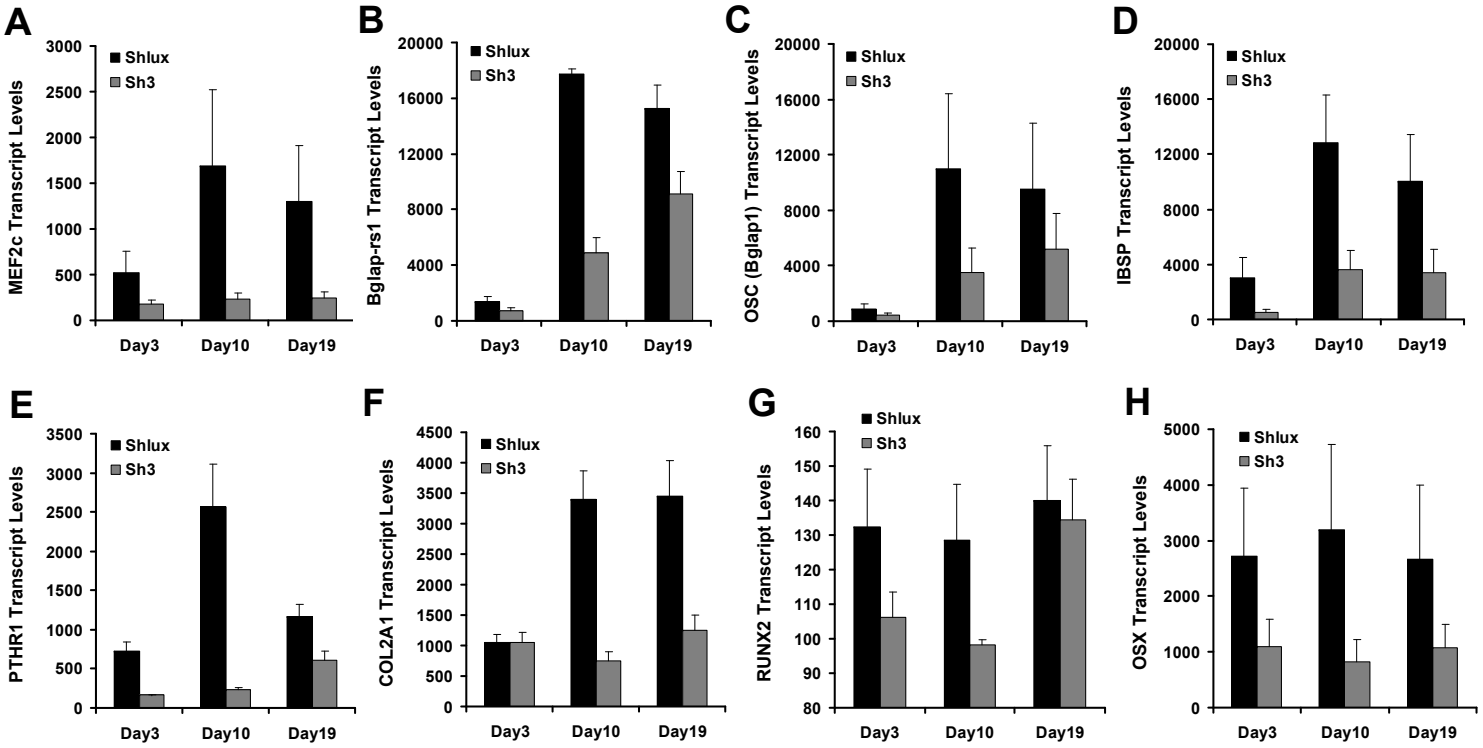

Figure 9 Stephens et al.